Electronic Supplementary Material (ESI) for RSC Advances.

Supporting Information

Li_2FePO_4F and its metal-doping for Li-ion batteries: An *ab initio* study

Fengmei Yang,[a] Weiwei Sun,[b] Yuhan Li,[a] Haiyan Yuan,[a] Zhiyong Dong,[a] Huanhuan Li,[a] Jumei Tian,[a] Yiying Zheng*, [a] Jingping Zhang,*[a]

[a] *Faculty of Chemistry, Northeast Normal University, Changchun 130024, China. E-mail: jpzhang@nenu.edu.cn.*
[b] *Department of Material Science and Engineering, KTH--Royal Institute of Technology, Department of Physics and Astronomy, Division of Material Theory, Uppsala University*

Available Information

S1: Electronic structure of Li_2FePO_4F/$LiFePO_4F$ polymorphs

S2: Stability of $Li_2Fe_{1-x}M_xPO_4F$ (M = Co, Mn)

S3: Two distinct positions for Fe in *Pnma*-Li_2FePO_4F.

S4: Volume changes of $Li_2Fe_{1-x}Co_xPO_4F$ (x = 1/8, 2/8, 3/8, 4/8, 5/8, 6/8, 7/8) upon delithiation.

S5: Migration barriers for diffusion of Li atom in the materials of $Li_2Fe_{1-x}Co_xPO_4F$ (x = 0, 0.25, 0.75).

S6: The electron localization function (ELF) of $Li_2Fe_{1-x}Co_xPO_4F$ (x = 0.25, 0.5, 0.75).

S1: Electronic structure of Li_2FePO_4F/$LiFePO_4F$ polymorphs

Fig. S1 shows the total density of states of Li_2FePO_4F/$LiFePO_4F$ and the values of band gaps. For all these three polymorphs of Li_2FePO_4F/$LiFePO_4F$, the Fermi level is between the highest occupied bands and the unoccupied 3*d* bands of Fe ions. Hence, the oxidation largely proceeds on Fe atoms when delithiated step.

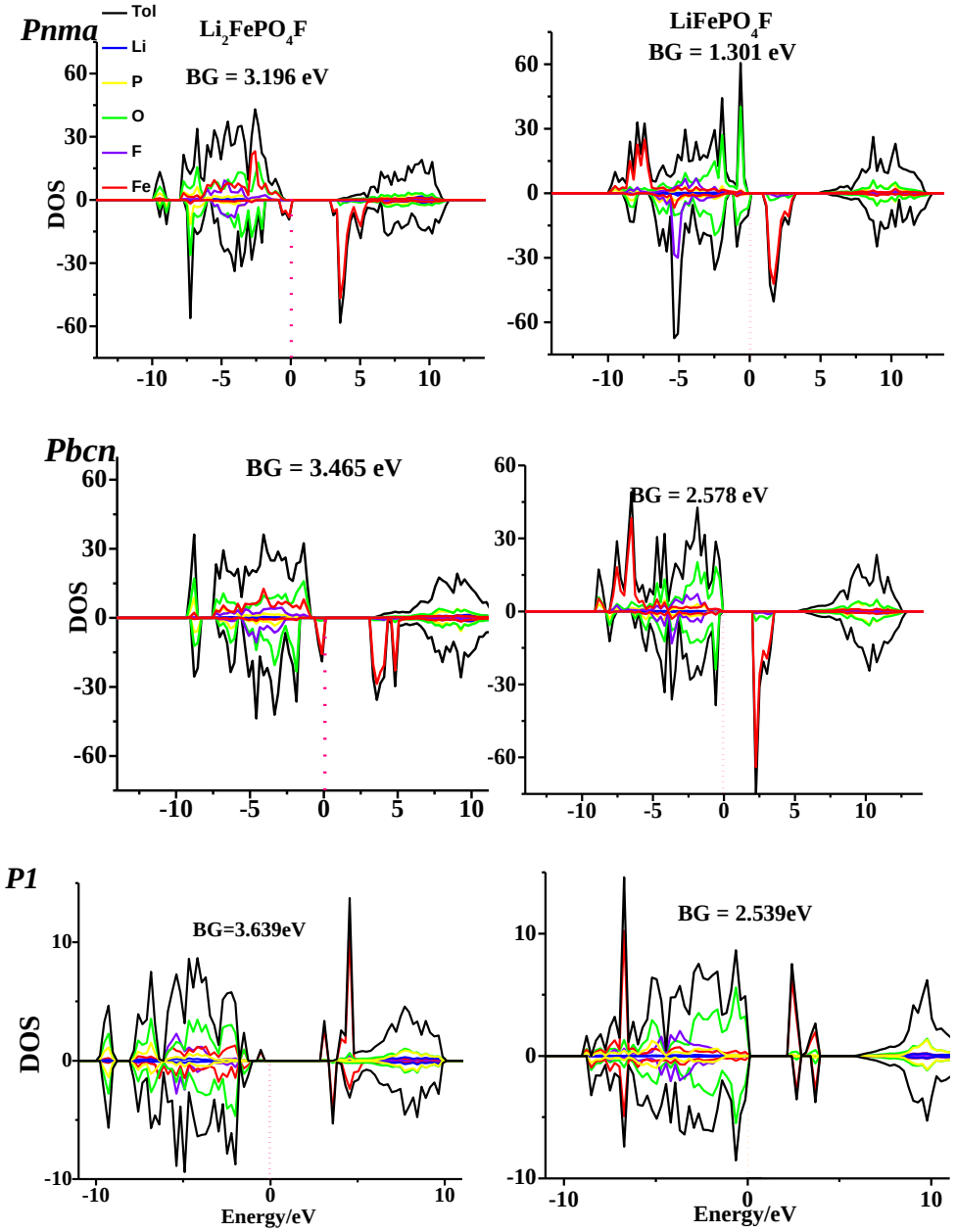

Fig. S1 The total density of states (DOS) of Li_2FePO_4F (left) and $LiFePO_4F$ (right); the Fermi level is set as a reference.

S2: Stability of $Li_2Fe_{1-x}M_xPO_4F$ (M = Co, Mn)

To investigate the stability of the Co/Mn—doped *Pnma*-Li_2FePO_4F, we calculated the formation energy of $Li_2Fe_{1-x}M_xPO_4F$ (M = Co/Mn, x = 1/8, 2/8, 3/8, 4/8, 5/8, 6/8, 7/8,1), as shown in Fig.S2. Their formation energy can be obtained from a total energy expression of (1) and (2)[1], where M = Co/Mn, E_{for} and E_{tol} denotes the formation energy and total internal energies respectively:

$$E_{for} = E_{tol}(\mathrm{Li_2Fe_{1-x}M_xPO_4F}) - xE_{tol}(\mathrm{Li_2MPO_4F}) - (1-\mathrm{x})E_{tol}(\mathrm{Li_2FePO_4F}) \quad (1)$$

$$E_{for} = E_{tol}(\mathrm{Li_2Fe_{1-x}M_xPO_4F}) - \mathrm{x}\,E_{tol}(\mathrm{LiMPO_4}) - (1-\mathrm{x})E_{tol}(\mathrm{LiFePO_4}) - E_{tol}(\mathrm{LiF}) \quad (2)$$

For example, for Eqn (1) the negative formation energy indicates that $Li_2Fe_{1-x}M_xPO_4F$ is stable enough with respect to phase separation into Li_2MPO_4F (M = Co/Mn) and Li_2FePO_4F, while the positive formation energies eliminated the existence of $Li_2Fe_{1-x}M_xPO_4F$ (M = Co/Mn). In Fig S2, hollow graphics correspond to the formation energy of $Li_2Fe_{1-x}M_xPO_4F$ as a function of Equ (1). It can be observed that the different doping contents, led to different values, whereas the absolute values of the obtained energies were relatively low. Hence, $Li_2Fe_{1-x}M_xPO_4F$ (M = Co/Mn) are stable enough for decompose to their parent compounds Li_2MPO_4F (M = Co/Mn) and Li_2FePO_4F. For Equ (2), we have to stress that the calculated formation energies of Li_2FePO_4F is positive, and consistent with the results of Ceder group (https://www.materialsproject.org/). But experimental studies revealed that Li_2FePO_4F is stable enough to be used as a cathode material in a Li-ion cell. For comparison, in Eqn (2), formation energy is relative to that of the un-doped Li_2FePO_4F, which formation energy is therefore set as the zero. In Fig S2, solid graphics correspond to the formation energy of $Li_2Fe_{1-X}M_xPO_4F$ as a function of Equ (2). For $Li_2Fe_{1-x}Mn_xPO_4F$ all of values are positive and high, which suggest that $Li_2Fe_{1-x}Mn_xPO_4F$ may decompose to $LiMnPO_4$, $LiFePO_4$ and LiF at the concentration of 12.5%, with $Li_2Fe_{0.875}Mn_{0.125}PO_4F$ at the least doping amount in our calculation. However the increasing addition of Co to Fe-based materials can improve the stability of $Li_2Fe_{1-x}Co_xPO_4F$. All the calculated results suggest that $Li_2Fe_{1-x}Co_xPO_4F$ is stable enough as a new cathode material and $Li_2Fe_{1-x}Mn_xPO_4F$ might easily resolve. This can be traced back to the isostructural of Li_2CoPO_4F with *Pnma*-Li_2FePO_4F, while Li_2MnPO_4F is different.

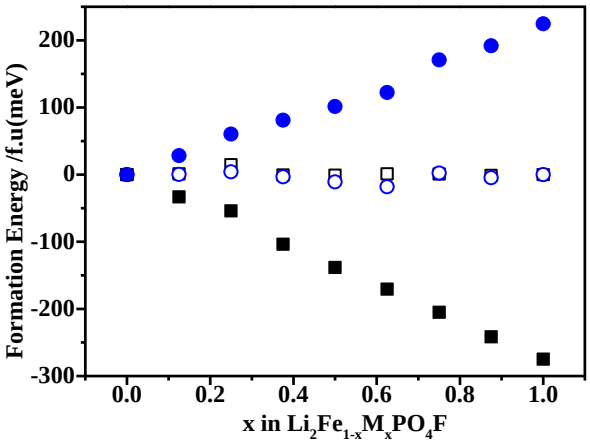

Fig. S2 The stability of $Li_2Fe_{1-X}Co_xPO_4F$ and $Li_2Fe_{1-X}Mn_xPO_4F$ (x = 1/8, 2/8, 3/8, 4/8, 5/8, 6/8, 7/8 and 1). Hollow graphics and solid graphics represent the formation energy of $Li_2Fe_{1-X}M_xPO_4F$ as a function of Equ (1) M = Co(hollow squares of black), Mn(hollow circle of blue) and Equ (2) M = Co(solid squares of black) M = Mn(solid circle of blue) respectively.

S3: Two distinct positions for Fe in *Pnma*-Li_2FePO_4F.

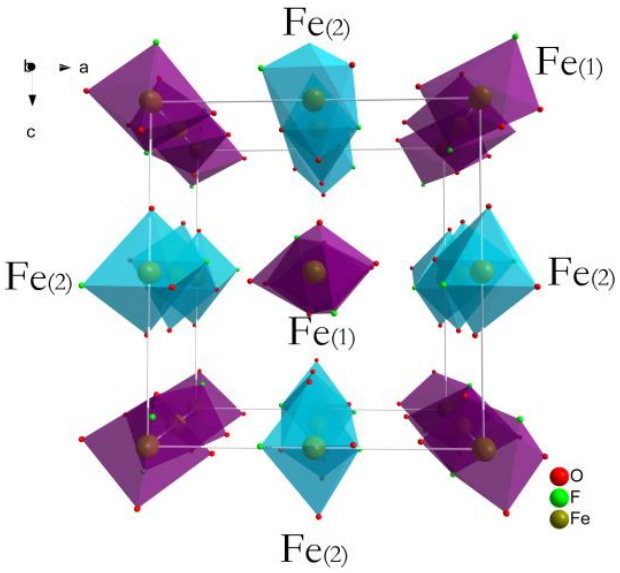

Fig. S3 Optimized crystal structures of *Pnma*-Li_2FePO_4F, violet octahedral: with TM at 4a sites (named $Fe_{(1)}$) for centre; sky blue: with TM at 4b sites (named $Fe_{(2)}$) for centre.

S4: Volume changes of $Li_2Fe_{1-x}Co_xPO_4F$ (x = 1/8, 2/8, 3/8, 4/8, 5/8, 6/8, 7/8) upon delithiation.

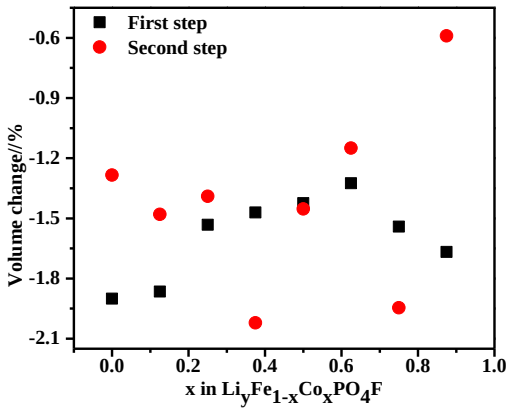

Fig. S4: Volume changes in $Li_2Fe_{1-x}Co_xPO_4F$-$LiFe_{1-x}Co_xPO_4F$ (First step) and $LiFe_{1-x}Co_xPO_4F$-$Fe_{1-x}Co_xPO_4F$ (Second step) (x = 1/8, 2/8, 3/8, 4/8, 5/8, 6/8, 7/8), (0.6%～2.1%), negative value means the unit cell volume contraction as Li^+ is removed.

S5: Migration barriers for diffusion of Li atom in the materials of $Li_2Fe_{1-x}Co_xPO_4F$ (x = 0, 0.25, 0.75).

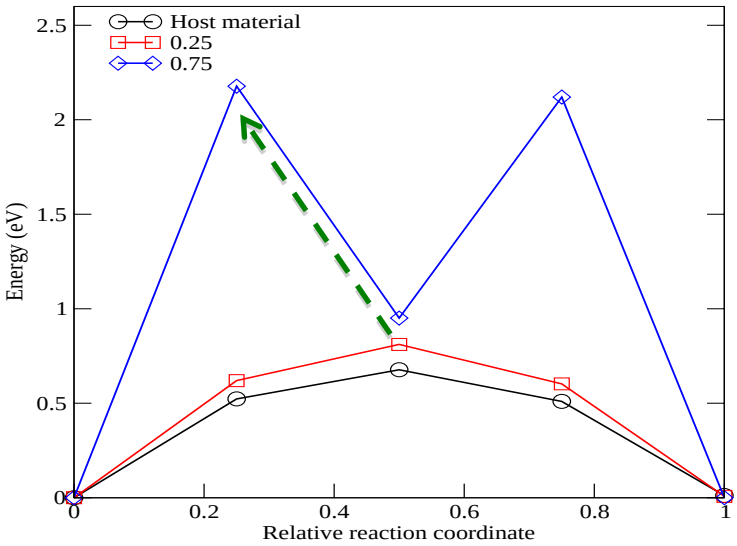

Fig. S5: The migration barriers for diffusion of Li in the materials of $Li_2Fe_{1-x}Co_xPO_4F$ (x = 0, 0.25, 0.75) along the [010] channel.

It was reported that there are two channels for Li diffusion, *i.e.*, [010] and [011][2]. However, the [010] channel has much "open" space as compared to [011]. Thus, [010] direction happens prior to the Li diffusion, and we only investigated the [010] channel by the DFT-based CI-NEB method. Considering the lack of computational source, we mainly focused on the effects of Co dopant on the Li diffusion and studied three images for $Li_2Fe_{1-x}Co_xPO_4F$ (x = 0, 0.25, 0.75) along the [010] channel. Fig.S5 shows that three images are enough, and they are capable of offering a clear trend in each case. The higher doping concentration leads to higher barrier. The Li atom in $Li_2Fe_{0.25}Co_{0.75}PO_4F$ has to overcome 2.17 eV to reach the ending point, while for the material of Li_2FePO_4F only needs 0.67 eV. As shown in Fig. 4, the unit cell volume of $Li_2Fe_{1-x}Co_xPO_4F$ should decrease with the substitution of Co for Fe, which is also supported by the stronger hybridization between Co-O in higher doping concentration shown in Fig. S6.

S6: The electron localization function (ELF) of $Li_2Fe_{1-x}Co_xPO_4F$ (x = 0.25, 0.5, 0.75).

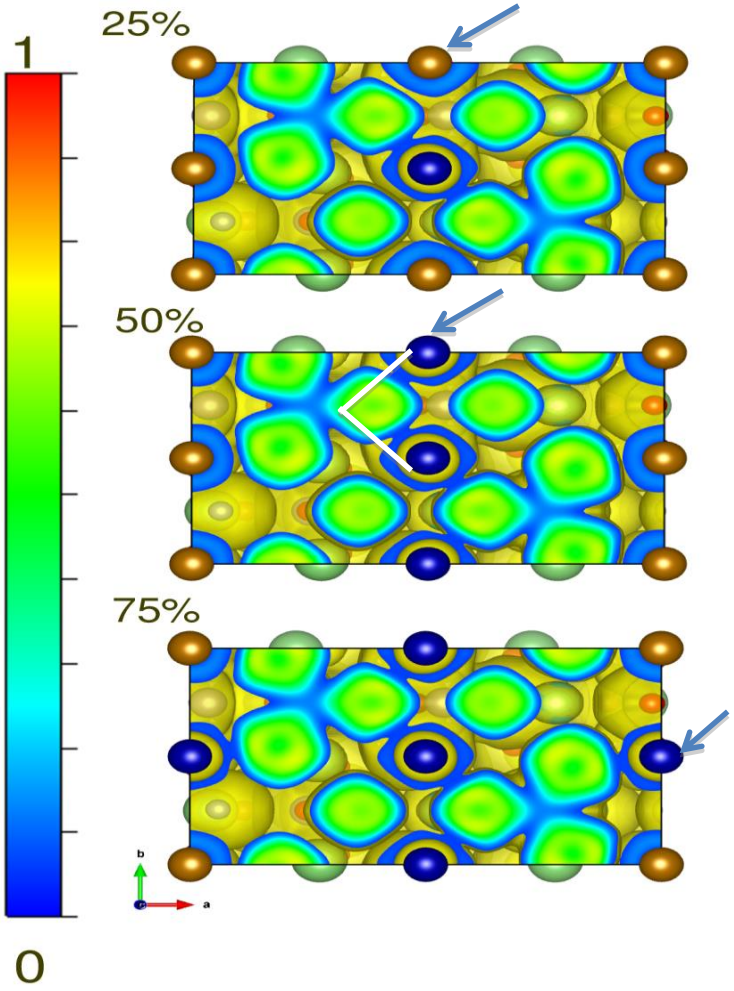

Fig.S6 The electron localization function (ELF) of the Li_2FePO_4F doped with Co by the concentration of 25%, 50%, and 75%. The golden balls represent Fe atoms, and blue ones for Co atoms. The level of isosurface in ELF is set to be 0.06.

To explain the hybridization of Co-3*d* and O-2*p* we performed the electron localization function (ELF) analysis of the Li_2FePO_4F doped with Co by the concentration of 25%, 50%, and 75% (Figure S6). The ELF is a scalar continuous function bounded between 0 and 1, and the value of 1 (red) indicates that electrons are fully localized and 0 (blue) implies that electrons are fully delocalized or that there is no electron in that place. The positions of the doped Co are set as the center of the square (25%), the vertical mirror plane (50%), and the horizontal mirror plane (75%). The doped concentration of 25% (see from the top of the square, as show by arrows) indicates that Co (blue) is more delocalized than Fe (light blue) because of the electron clouds around Co and the O atoms forming a bridge-like tunnel and increasing the probability of charge transfer. When

the doping rate is lower than 50%, the hybridization states broadening from -6 eV to -2 eV, while the doping rate arises from 50% to 75%, the evident hybridization peaks gradually change from -2 eV to -4 eV. It is well known that in the TMO systems, the orientation of *d* orbital plays a significant role on the *d-p* hybridization. When the doping rate is 50%, the orientations of Co-O bonds are symmetric as the red lines indicate. However, if the doping rate reaches at 75%, the orientation has been changed.

1. A. Yamada, N. Iwane, S.-i. Nishimura, Y. Koyama and I. Tanaka, *Journal of Materials Chemistry*, 2011, **21**, 10690-10696.
2. N. R. Khasanova, O. A. Drozhzhin, D. A. Storozhilova, C. Delmas and E. V. Antipov, *Chemistry of Materials*, 2012, **24**, 4271-4273.
3. R. Long and N. J. English, *Chemistry of Materials*, 2010, **22**, 1616-1623.